文章编号：0258-8013 (2008) 10-0037-09　　中图分类号：TM 71　　文献标识码：A　　学科分类号：470·40

一种新的水火电力系统优化潮流模型

哈比比，余贻鑫

(天津大学电气与自动化工程学院，天津市 南开区 300072)

A Novel Formulation of Optimal Hydrothermal Power Flow

Alhabib BINKOU, YU Yi-xin

(School of Electrical Engineering and Automation, Tianjin University, Nankai District, Tianjin 300072, China)

ABSTRACT: A formulation of optimal hydrothermal power flow (OHPF) problem is presented. Fuel cost and emissions objective are included in the formulation. The transmission loss is approximately expressed in terms of the generalized generation shift distribution factor (GGDF) and of generated power, the dynamic security region (DSR) to guarantee the transient stability constraints and static voltage stability region (SVSR) constraints are included as constraints. The trade-off relation between fuel cost and emissions is also studied. The Jacobian matrix is formulated by incremental transmission loss in terms of the sensitivity factors, the DSR constraints, and the SVSR constraints. The implementation is based on a Newton Raphson's interactive procedure, with novel initial guesses to obtain improved convergence properties. Two standard systems are worked out in order to demonstrate the effectiveness of the proposed method.

KEY WORDS: hydrothermal power systems; emissions; generalized generation shift distribution factors; trade-off relation; security regions

摘要：提出了一种新的水火电力系统的优化潮流模型，该模型以最小化燃料费用和污染排放量为目标。模型中的约束条件考虑了网损和系统稳定性 2 个方面，其中网损用发电量和发电量转移分配系数表示，系统的暂态稳定性和静态电压稳定性分别用动态安全域和静态电压稳定域的方式表示。该文还就目标函数中考虑燃料费用和污染排放比例关系进行了研究。优化模型的雅克比矩阵由网损和各节点发电量之间的灵敏度因子以及动态安全域和静态电压安全域的系数构成。该模型的求解使用牛顿–拉夫逊迭代法实现，并采用一种新的初值设定方法以提高计算的收敛特性。通过 2 个标准系统算例验证了该模型的有效性。

基金项目：国家自然科学基金项目(50595413)；国家重点基础研究发展计划项目(973 项目) (2004CB217904)。

Project Supported by National Natural Science Foundation of China (50595413); The National Basic Research Program of China (973 Program) (2004CB217904)。

关键词：水火电力系统；污染排放；发电量转移分配系数；比例关系；安全域

0 INTRODUCTION

The conventional formulation of the optimal hydrothermal power flow (OHPF) is designed to minimize the fuel cost for thermal plants under the constraints of the water available for hydro generation in a given period of time. The OHPF is one of fruitful applications of OPF, which is more realistic than conventional OPF because of dynamic coupling between the variables of the problem as a result of the hydro energy constraints introduced through the volume of water availability limitations [1-11]. Therefore, it is very challenging to develop an efficient algorithm for OHPF. Several algorithms have been introduced in recent years for solving the objective of the OHPF problem, including genetic algorithm [2], dynamic programming [3-4], simulated-annealing techniques and parallel simulated-annealing approach [5], stochastic and aggregation linear programming [6], and fast evolutionary programming techniques [7]. However, it is difficult to apply them in real-time power system dispatching due to their computation burden. The conventional Newton Raphson method is simple, however the divergence possibilities associated to this method have been pointed out in Ref. [8]. More recently, interior point method has been applied to this topic to enhance the computational efficiency and to reduce the memory requirement [9-10]. However, the interior point method does not reduce the size of the correction

equation of the OHPF and the solution of the complementary gap of approximate OHPF problem (A-OHPF) is not optimal, yet it may not converge to the OHPF. Moreover the above formulation of OHPF did not take into account the transmission losses in its minimization, and the transient stability and voltage stability in its constraints. The effects of load modeling on minimum loss, minimum emission, and multiple-objective optimal hydrothermal power flow have been investigated in Ref. [11]. However, the transient stability and voltage stability constraints have not been considered in the study.

Fossil-fired electric power plants use coal, oil, gas or combinations thereof as the primary energy resource, and produce atmospheric emissions whose nature and quantity depend on the fuel type and its quality. Coal produces particulate matter such as ash, and gaseous pollutants such as carbon oxides (CO_2), sulfur oxides (SO_2) and oxides of nitrogen (NO_x). The major part of electric power generation is due to fossil-fired plants and their emissions contribution cannot be neglected. Pollution affects not only humans, but also other life-forms such as animals, birds, fish, and plants. It also causes damage to materials, reducing visibility, as well as causing global warming. These effects may be interpreted as costs because they damage our life in one way or another. In order to meet environment regulations, emission control has become one of most important operational objectives. Including emissions in the objective function was reported in many publications [11-13]. A summary of environmental/economic dispatch algorithms has been reported in Ref. [12]. Ref. [13] proposes the surrogate worth trade-off approach for multiobjective thermal power dispatch problem. Existing multiple-objective minimization algorithms do not take into account the transient stability constraints and voltage stability constraints.

Some algorithms are found in the literature dealing with power system losses calculation [14-15]. The conventional method to calculate the power losses from the *B*-coefficients is still widely used for real-time economic dispatch of the power systems [14]. However, the *B*-coefficients are not constant for all different operating points and this will affect the solution accuracy. Ref. [15] proposes A_i-factors to improve *B*-coefficients method. This method eliminates many assumptions and detours complicated calculations, yet it requires running load flow many times and the loss coefficients result in poor accuracy when they are applied to different load levels [16].

In this paper a novel formulation of the optimal hydrothermal power flow problem is suggested with taking into account the emissions minimization, and the transient stability and voltage stability in its constraints based on the concepts of security regions [17]. The algorithm is based on a Newton Raphson's method. In order to speed up the computation of the OHPF, a novel initial guesses and LU factorization corresponding to a permutation of the rows of Jacobian matrix (Lagrange matrix) at each iteration are suggested. To overcome the deficiencies of the *B*-coefficients and A_i-factors, the transmission loss is expressed in terms of the GGDF and generated power [16]. Trade-off relations between fuel cost and emissions are studied in the simulations reported. The proposed method is tested on two IEEE test systems and satisfactory results reported.

1 THE OHPF FORMULATION

1.1 Objective Function

Fuel cost and emissions are conflicting objectives and cannot be minimized simultaneously. However, non-inferior solutions may be obtained in which fuel cost and emissions are combined in a single function with different weightings. For a specified demand, a trade-off curve may then be obtained. Any point on this curve is considered to be feasible solution with specific values of fuel cost and emissions. This objective function is described by:

$$\min \quad C_T = wC_F + (1-w)E \tag{1}$$

Subject to equality constraints, inequality constraints, transient stability constraints and voltage stability constraints. C_F is the total fuel cost function with weighting w, E is the total combined emissions function with weighting $(1-w)$. The weighting satisfies

$0 \le w \le 1$. If $w = 1.0$ the solution is that of minimum fuel cost, and if $w = 0$ the solution is minimum emissions. The goal of the objective function is to find an operating point that will minimize the generation cost and the system emissions simultaneously. Let's assume that the system consists of N_G generating plants, among which N_H are hydro fixed head plants, and N_S thermal plants, N buses, and N_L transmission lines.

The fuel cost component C_F over the optimization interval [0, T_f], is the conventional objective function defined by:

$$C_F = \int_0^{T_f} \{\sum_{i=1}^{N_S} [a_i + b_i P_{gi}(t) + c_i P_{gi}^2(t)]\} \mathrm{d}t \qquad (2)$$

Where a_i, b_i and c_i are the fuel cost parameters of the generating source at the i^{th} bus. The emission function E is the sum of all types of emissions considered such as NO_x, SO_2, etc with suitable pricing on each. This function may be represented as:

$$E = C_{\mathrm{NO}_x} \cdot E_{\mathrm{NO}_x} + C_{\mathrm{SO}_2} \cdot E_{\mathrm{SO}_2} + ... \qquad (3)$$

Where C_{NO_x} and C_{SO_2} are respectively the price on NO_x emission and SO_2 emission. E_{NO_x} and E_{SO_2} are respectively the NO_x emission function and SO_2 emission function. Each price represents the degree of harmfulness of the emissions type. Assigning a price to emission depends on its biological and ecological effects. The emission function E over the optimization interval [0, T_f] given as follows [11-12]:

$$E = \int_0^{T_f} \{\sum_{i=1}^{N_S} [d_i + e_i P_{gi}(t) + f_i P_{gi}^2(t)]\} \mathrm{d}t \qquad (4)$$

Where d_i e_i and f_i are the emission parameters and assumed to be known for each of thermal plant units in the system, and P_{gi} is active power generation at unit i. No emissions or fuel cost is associated with the operation of a hydro unit. Since the time period $[0, T_f]$ is about 15 minutes to half hour, it is an OPF problem.

1.2 Equality Constraints

The total system generation matches power demand $P_D(t)$ and the transmission losses $P_L(t)$:

$$\sum_{i=1}^{N_S} P_{gi}(t) + \sum_{j=1}^{N_H} P_{gj}(t) = P_D(t) + P_L(t) \qquad (5)$$

The prespecified volume of water (say Q_j) available at each hydro plant for power generation is as follows:

$$\int_0^{T_f} q_j(t) \mathrm{d}t = Q_j, \quad j = 1, 2, ..., N_H \qquad (6)$$

The hydraulic performance for short period dispatch proposed by Glimn-Kirchmayer is a quadratic function in terms of the active power generation [8].

$$q_j[P_{gj}(t)] = \alpha_j + \beta_j P_{gj}(t) + \gamma_j P_{gj}^2(t), \ j = 1, 2, ..., N_H \qquad (7)$$

Where α_i, β_i and γ_i are assumed to be known for each of the hydro plant units in the system, q_j is water discharge of hydro plant j, and P_{gj} is the active power generation at hydro-electrical power generator bus j.

1.3 Inequality Constraints

The inequalities on the problem variables considered are:

Upper and lower bounds on the active power generations at generator bus:

$$P_{gi}^{\min} \le P_{gi} \le P_{gi}^{\max}, \quad i = 1, 2, ..., N_G \qquad (8)$$

Line flow constraints:

$$P_m \le P_m^{\max}, \quad m = 1, 2, ..., N_L \qquad (9)$$

Where P_m is the magnitude of the active power flow in the m^{th} line.

1.4 Security Region Constraints

The security regions (SR) defined in injection space is unique for a given power system configuration or a power system with a particular postulated change in configuration. Two types of security regions have been considered: DSR to guarantee transient stability and static security region (SSR) to guarantee static voltage stability.

（1）Static voltage stability region constraints. It has been found that the critical boundary of SVSR can be expressed by a hyper-plane [18-19] as follows:

$$\sum_{i \in N_{\mathrm{CS}}} a_i P_i \le 1 - \varepsilon \qquad (10)$$

Where CS is a critical cut-sets, and P_i is the active power flow of branch i in the critical cut-set, coefficients a_i ($i \in N_{\mathrm{CS}}$) describe the "weight" of the impact of branch i in the critical cut-set on static voltage stability, the number of branches in critical cut-set is usually a small number, and ε is a small

constant ($\varepsilon \approx 0.1$) that represents necessary margin.

（2）Transient stability constraints. It has been found that the critical boundary of DSR can be approximately expressed as a hyper-plane in large range in injection space as follows [20]:

$$\sum_{i\in G\cup L_D} \alpha_i^j P_i \le 1-\varepsilon, \quad \forall j \in \{\text{contigency set}\} \tag{11}$$

Where α_i^j is the i^{th} node coefficient of critical hyper-plane corresponding the j^{th} fault, P_i is real power injection at bus i, G and L_D denote the set of generators buses and the set of load buses respectively, and ε is a small constant ($\varepsilon \approx 0.1$) that represents necessary margin.

2 ACTIVE POWER LOSS

The relationship among the active power loss, line flow and unit generation can be expressed in terms of the GGDF. Under the direct current (DC) approximation of load flow, the power loss of line m can be expressed in terms of resistance and line flow as follows:

$$P_{Lm} = R_m P_m^2, \quad m = 1,2,...,N_L \tag{12}$$

The system power loss is expressed by the summation over all transmission line as follows:

$$P_L = \sum_{m=1}^{N_L} R_m P_m^2 \tag{13}$$

Where R_m and P_m are respectively the resistance and active power flow of transmission line m.

The use of sensitivity method to compute line flows in system security and contingency analysis remains very popular. The excellent properties of simplicity, linearity, accuracy and rapidity computation make it widely acceptable in on-line application.

The generation shift distribution factor (GSDF) $A(m,i)$ can be used to calculate line flow when the total system generation remains unchanged. We can calculate the GSDF using the definition of the reactance matrix and the DC approximation of load flow [21].

$$A(m,i) = \frac{\partial P_m}{\partial P_{Gi}} = \left(\frac{\partial \theta_l}{\partial P_{Gi}} - \frac{\partial \theta_k}{\partial P_{Gi}}\right) / X_m = \frac{X_{li} - X_{ki}}{X_m}$$
$$m = 1,2,...,N_L \tag{14}$$

Where X_{li} and X_{ki} are the components of the reactance matrix $\boldsymbol{X}$ of DC load flow equation; l and k are the sending and the ending buses of line m respectively.

When the total system generation changes, the GGDF should be used to calculate the line flows. The GGDF of line m due to generator i, $D(m,i)$ can be used to calculate the line flow. It can be defined by the following equation [22]:

$$P_m = \sum_{i=1}^{N_G} D(m,i) P_{Gi}, \quad m = 1,2,...,N_L \tag{15}$$

The GGDF can be calculated as follows:

$$\begin{cases} D(m,i) = D(m,r) + A(m,i) \\ D(m,r) = \dfrac{P_{m0} - \sum\limits_{i\ne r, i=1}^{N_G} A(m,i) P_{Gi}}{\sum\limits_{j=1}^{N_G} P_{Gj}} \end{cases} \tag{16}$$

Where $D(m,r)$ is the GGDF for line m due to generator r, r is the reference bus and P_{m0} denotes the initial line flow on line m.

By substituting Equ.(15) and (16) into Equ. (13), the active power loss of the whole system can be formulated as follows:

$$P_L = \sum_{m=1}^{N_L} \{R_m [\sum_{i=1}^{N_G} D(m,i) P_{Gi}]^2\} \tag{17}$$

3 COORDINATION EQUATION

The total cost (1) is attempted to be minimized for a given value of the weighting factor subject to system constraints. The Lagrange multiplier method is used to find the solution of the optimal objective hydrothermal power flows problem; the new objective function L can be expressed as follows:

$$\begin{aligned} L = {} & C_T - \lambda_g [\sum_{i=1}^{N_S} P_{gi}(t) + \sum_{j=1}^{N_H} P_{gj}(t) - P_D(t) - P_L(t)] + \\ & \sum_{i=1}^{N_H} \nu_i [\int_0^{T_f} q_i(t) \mathrm{d}t - Q_i] + \sum_{i=1}^{N_G} \pi_i^{\min} [P_{gi}^{\min} - P_{gi}] + \\ & \sum_{i=1}^{N_G} \pi_i^{\max} [P_{gi} - P_{gi}^{\max}] + \sum_{k=1}^{M_L} \mu_k [P_k - P_k^{\max}] + \\ & \sum_{i=1}^{N_G} \delta_i [\sum_{i\in G} \alpha_i^j P_{gi} - (1 - \varepsilon - \sum_{i\in L_D} \alpha_i^j P_i)] + \\ & \sum_{i=1}^{N_G} \sigma_i [\sum_{i\in N_{CS}} a_i P_i - (1-\varepsilon)] \end{aligned} \tag{18}$$

Where M_L denotes a set of the overload transmission

lines. $\lambda_g, \nu_i, \pi_i^{\min}, \pi_i^{\max}, \delta_i$, σ_i and μ_k represented the Lagrange multiplier for the power balance constraint, the hydraulic power generation constraint, the active power generation inequality constraints, the DSR constraints, the SVSR constraints and the constraints of all overload transmission lines respectively. The necessary condition of minimizing L is that the partial differentiation of Equ. (18) with respect to P_{gi}, λ_g, ν_i, $\pi_i^{\min}, \pi_i^{\max}, \delta_i$, σ_i and μ_k should be zero i.e.:

$$f_{si} = \frac{\partial L}{\partial P_{gi}} = t_p w \frac{\partial C_F}{\partial P_{gi}} + t_p (1-w) \frac{\partial E}{\partial P_{gi}} - \lambda_g (1 - \frac{\partial P_L(t)}{\partial P_{gi}}) - \pi_i^{\min} + \pi_i^{\max} + \delta_i \sum_{i=1}^{N_S} \alpha_i^j + \sigma_i a_h D(h,i) + \mu_k D(k,i) = 0, \ i = 1,2,...,N_S \quad (19)$$

$$f_{hi} = \frac{\partial L}{\partial P_{gi}} = -\lambda_g (1 - \frac{\partial P_L(t)}{\partial P_{gi}}) + t_p \nu_i (\beta_i + 2\gamma_i P_{gi}) - \pi_i^{\min} + \pi_i^{\max} + \delta_i \sum_{i=1}^{N_H} \alpha_i^j + \sigma_i a_h D(h,i) + \mu_k D(k,i) = 0, \quad i = 1,2,...,N_H \quad (20)$$

$$g_{\lambda_g} = \frac{\partial L}{\partial \lambda_g} = P_D(t) + P_L(t) - \sum_{i=1}^{N_S} P_{gi}(t) - \sum_{j=1}^{N_H} P_{gj}(t) = 0 \quad (21)$$

$$h_{vi} = \frac{\partial L}{\partial \nu_i} = \int_0^{T_f} (\alpha_i + \beta_i P_{gi}(t) + \gamma_i P_{gi}^2(t)) \, \mathrm{d}t - Q_i = 0, \quad i = 1,2,...,N_H \quad (22)$$

$$h_{\pi i^{\min}} = \frac{\partial L}{\partial \pi_i^{\min}} = P_{gi}^{\min} - P_{gi} = 0, \quad i = 1,2,...,N_G \quad (23)$$

$$h_{\pi i^{\max}} = \frac{\partial L}{\partial \pi_i^{\max}} = P_{gi} - P_{gi}^{\max} = 0, \quad i = 1,2,...,N_G \quad (24)$$

$$h_{\delta i} = \frac{\partial L}{\partial \delta_i} = \sum_{i \in G} \alpha_i^j P_{gi} - (1 - \varepsilon - \sum_{i \in L_D} \alpha_i^j P_i) = 0, \quad j \in \{\text{contengency set}\} \quad (25)$$

$$h_{\sigma i} = \frac{\partial L}{\partial \sigma_i} = a_h D(h,i) P_{gi} - (1-\varepsilon) = 0, \quad i = 1,2,...,N_G; \ h \in N_{\mathrm{CS}} \quad (26)$$

$$h_{\mu k} = \frac{\partial L}{\partial \mu_k} = P_k - P_k^{\max} = 0, \ k = 1,2,...,M_L \quad (27)$$

Where t_p is the length of the p^{th} interval of time, the term $(\partial P_L / \partial P_{gi})$ is the incremental transmission loss (ITL).

The solution of Equ.(19) gives optimum active thermal power generations and the convergence of the solution is dependent on the prudent selection of λ_g. From Equ. (2), (4), (17) and (19), we obtain the output of the i^{th} thermal generation unit as follows:

$$P_{gi} = \frac{\lambda_g (1 - ITL_i) - [wb_i + (1-w)e_i]}{2[wc_i + (1-w) f_i]}, \ i = 1,2,...,N_S \quad (28)$$

By substituting Equ. (1), (5) and (17) into Equ. (28), the Lagrange multiplier λ_g can be expressed as follows:

$$\lambda_g = \frac{2(P_D + P_L - \sum_{j=1}^{N_H} P_{gj}) + \sum_{i=1}^{N_S} \frac{wb_i + (1-w)e_i}{wc_i + (1-w) f_i}}{\sum_{i=1}^{N_S} \frac{1 - ITL_i}{wc_i + (1-w) f_i}} \quad (29)$$

The active power generation from the hydraulic unit is assumed to be constant for each time interval. The initial active power generation is the positive root of the quadratic formula (22).

$$P_{gik} = \frac{-\beta_i + \sqrt{\beta_i^2 - 4\gamma_i(\alpha_i - q_{ik})}}{2\gamma_i}, \quad i = 1,2,...,N_H; \ \ k = 1,2,...,N_T \quad (30)$$

Where q_{ik} is the discharge of the volume of water at the k^{th} time interval, N_T is a set of interval period.

The initial value for the water conversion coefficients is determined by substituting Equ. (17) in Equ. (20):

$$\nu_i = \frac{\lambda_g (1 - ITL_i)}{\beta_i + 2\gamma_i P_{gi}}, \quad i = 1,2,...,N_H \quad (31)$$

The approach algorithm is based on a Newton-Raphson's method, and the LU factorization corresponding to a permutation of the rows of Jacobian matrix (Lagrange matrix) to obtain improved convergence. The Jacobian matrix can be obtained as follows:

$$\Delta \boldsymbol{F} = \boldsymbol{J} \Delta \boldsymbol{X} \quad (32)$$

Where

$$\Delta \boldsymbol{F} = [\Delta f_s, \Delta f_h, \Delta g_{\lambda_g}, \Delta h_{\nu}, \Delta h_{\pi^{\min}}, \Delta h_{\pi^{\max}}, \Delta h_{\delta}, \Delta h_{\sigma}, \Delta h_{\mu}]^{\mathrm{T}}$$

$$\Delta \boldsymbol{X} = [\Delta P_{gs}, \Delta P_{gh}, \Delta \lambda_g, \Delta \nu, \Delta \pi^{\min}, \Delta \pi^{\max}, \Delta \delta, \Delta \sigma, \Delta \mu]^{\mathrm{T}}$$

The Jacobian matrix structure of Equ. (32) can be written in the partitioned form as follows:

$$\boldsymbol{J} = \begin{bmatrix} \boldsymbol{A} & \boldsymbol{B} \\ \boldsymbol{C} & 0 \end{bmatrix}$$

Where $\boldsymbol{A}$ is the Hessian matrix of the Lagrangian function with respect to the generations of all units. $\boldsymbol{C}$=$\boldsymbol{B}^{\mathrm{T}}$ is the matrix whose rows are the gradients of the

constraints Equ.(5), (6), (8), (9),(10) and (11). The solution steps based on the proposed algorithm, which simultaneously includes the DSR constraints, the SVSR constraints, the power generation constraints, the power balance constraints, the volume of available water constraints and the constraints of all line flow are summarized as follows.

（1）Read system data.

（2）Calculate reactance matrix $\boldsymbol{X}$.

（3）Calculate the GSDF (14) and the GGDF (16).

（4）Calculate the coefficients of cut-set a_i (10).

（5）Compute the coefficients of critical hyper-plane α_i^j (11).

（6）Compute the real power P_m of every transmission line and the transmission loss P_L.

（7）Calculate initial values of λ_g (29), ν (31), P_{gs} thermal generation (28) and P_{gh} hydro generation (30).

（8）Calculate the Jacobian matrix (32).

（9）Solve $\Delta P_{gs}, \Delta P_{gh}, \Delta\lambda_g, \Delta\nu, \Delta\pi^{\min}, \Delta\pi^{\max}, \Delta\delta$ and $\Delta\sigma$ (32).

（10）Check $\Delta P_{gs}, \Delta P_{gh}, \Delta\lambda_g, \Delta\nu, \Delta\pi^{\min}, \Delta\pi^{\max}, \Delta\sigma$ and $\Delta\delta$ whether converge or not (say $\|x\|_\infty \le \varepsilon$) where ε is prespecified tolerance.

（11）If all $\Delta P_{gs}, \Delta P_{gh}, \Delta\lambda_g, \Delta\nu, \Delta\pi^{\min}, \Delta\pi^{\max}, \Delta\delta$ and $\Delta\sigma$ converge while satisfying the inequalities, compute $F(x)$ and checks its convergence (say $\|F\|_\infty \le \varepsilon$). If $F(x)$ convergences, go to end.

（12）Update $\Delta P_{gs}, \Delta P_{gh}, \Delta\lambda_g, \Delta\nu, \Delta\pi^{\min}, \Delta\pi^{\max}, \Delta\delta$ and $\Delta\sigma$ and check constraint violations.

（13）If no constraint violations occur, go to Step（6）; otherwise for constraint violations go to next step.

（14）Calculate the GSDF and GGDF for the overloaded line.

（15）solve $\Delta P_{gs}, \Delta P_{gh}, \Delta\lambda_g, \Delta\nu, \Delta\pi^{\min}, \Delta\pi^{\max}, \Delta\delta, \Delta\sigma$ and $\Delta\mu$ (32); go to Step（10）.

（16）Prints results.

4 TEST RESULTS AND DISCUSIONS

The proposed algorithm has been applied on the sample IEEE 14 and 30-bus systems. The test systems characteristics and system capacity (say base case) are listed in Tab.1, while their generation specifications and emission coefficients are listed in Tab.2 and Tab. 3 respectively.

Tab.4 provides branches, which define the cut-set and the coefficients of equation (10) for the two test systems.

表 1 算例系统特性

Tab. 1 Characteristics of the test systems

Test systems	IEEE 14-bus	IEEE 30-bus
Buses	14	30
Lines	20	41
Thermal units	2	2
Hydraulic units	1	1
System capacity (base case) /MW	259.0	283.4

表 2 发电费用系数

Tab. 2 Generation specifications

Test systems	Bus	α	β	γ	Q
IEEE 14-bus system	1	35.550	9.990	0.014 00	100.00
	2	0.360 0	0.071 9	$0.774\,5\times10^{-4}$	
	3	35.330	10.990	0.014 06	
IEEE 30-Bus system	1	118.607	9.662 0	$0.116\,5\times10^{-2}$	100.00
	2	0.360 0	0.071 9	$0.774\,5\times10^{-4}$	
	13	118.607	9.200 0	$0.116\,5\times10^{-2}$	

表 3 污染排放系数

Tab. 3 Emission coefficients

Test systems	Bus	d	e	f
IEEE 14-bus	1	132.279 7	4.678 00	0.007 529
	3	211.085 4	3.055 97	0.008 803
IEEE 30-Bus	1	832.698 2	3.095 86	0.004 458
	13	171.594 1	3.758 61	0.009 759

表 4 电压稳定域的边界系数

Tab. 4 Coefficients of the boundary of the SVSR

Test system	Cut-set	Coefficients
IEEE 14-bus system	6-12	−0.036 05
	6-13	0.002 879 5
	13-14	−0.001 39
IEEE 30-bus system	23-24	0.007 936 9
	8-28	−0.012 13
	6-28	0.011 302

Six 3-phase to ground short circuit faults are considered in this study. The faults will be cleared after the duration τ=0.1 second and the faulted transmission line is to be open in the post-fault configuration. The DSRs usually depend on operator's purpose or pre-analysis of the system structure and fault location and type. Power injections nodes and their coefficients of the hyper-planes are shown in Tab.5 and Tab.6 for the 14 and 30-bus systems

respectively for different fault lines.

The load demand for the dispatch period is considered to be the peak load for a quarter and half load for the next quarter.

Tab.7 lists the desired optimal schedules for the generating units' active power, active power loss, energy loss, the water worth factor that are associated with the different loads and the CPU times.

It is observed that the transmission power losses and the energy loss differ for the test system in every time interval. In all systems considered, the power losses increase during the high demand period, and decrease during the low demand period. The proposed method has been implemented on a Pentium IV computer with 2.40 GHz and 256 MB RAM. The proposed method is 15 and 25 times faster than the conventional Newton method for the IEEE 14 and 30-bus systems respectively.

Results for different compromise factor w varied in steps of 0.1 in the entire range of $0 \le w \le 1$ in terms of emissions and fuel cost are given in Tab. 8 and Tab. 9 for the 14 and 30-bus systems respectively. Tab. 8 and Tab. 9 list a comparison of the results when the security constraints are considered. With security constraints, when w is increased from 0~1.0, it is seen

表 5　IEEE 14 母线系统动态安全域的边界系数
Tab. 5　Coefficients of the boundary of the DSR for IEEE 14-bus system

Events powers	P_{g1}/pu	P_{g2}/pu	P_{g3}/pu
1-5	0.009 5	–0.503 3	0.005 85
2-3	0.006 6	–0.928 9	–1.113 06
2-4	0.001 8	–0.459 7	0.104 66
3-4	0.001 9	–0.366 6	0.061 55
10-11	0.001 3	–0.400 7	0.157 82
13-14	0.001 7	–0.391 8	0.025 84

表 6　IEEE 30 母线系统动态安全域的边界系数
Tab. 6　Coefficients of the boundary of the DSR for IEEE 30-bus system

Events powers	P_{g1}/pu	P_{g2}/pu	P_{g3}/pu
1-2	0.009 3	–1.364 2	–1.227 6
1-3	0.007 1	–0.654 8	–0.915 5
2-4	–0.025 9	–0.465 9	–0.827 4
2-5	0.000 4	–0.550 0	–0.887 4
2-6	–0.025 9	–0.465 9	–0.827 4
4-6	–0.019 8	–0.599 1	–0.685 0

表 7　优化计算结果
Tab. 7　Results of optimization

Test systems		System load I: 100% of base case	System load II: 50% of base case
IEEE 14-bus	P_{g1}/MW	157.559	81.342
	P_{g2}/MW	105.417	50.529
	P_{g3}/MW	11.398	6.993
	P_L/MW	15.374	9.364
	E_L/(MW·h)	23.061	14.046
	ν	0.993	0.872
	CPU time/s	5.472	2.964
IEEE 30-bus	P_{g1}/MW	133.255	86.104
	P_{g2}/MW	92.533	41.413
	P_{g3}/MW	68.634	22.427
	P_L/MW	11.022	8.244
	E_L/(MW·h)	16.533	12.366
	ν	52.433	20.409
	CPU time/s	7.286	3.893

表 8　IEEE 14 节点系统取不同 *w* 值(0~1.0)所对应的污染排放量和燃料费用优化结果
Tab. 8　Emissions and fuel cost *w* varies from 0.0 to 1.0 in increments of 0.1 for IEEE 14-bus system

w	Without security region constraints		With security region constraints	
	Emissions/(kg/h)	Fuel cost/($/h)	Emissions/(kg/h)	Fuel cost/($/h)
0.0	61 665.044	141 761.011	119 930.512	182 140.663
0.1	61 714.856	141 600.505	119 965.612	182 050.665
0.2	61 801.262	141 398.104	120 124.854	181 880.282
0.3	61 868.296	141 284.525	120 212.113	181 760.367
0.4	61 928.448	141 204.595	120 305.303	181 600.778
0.5	61 996.841	141 040.105	120 408.484	181 500.227
0.6	62 089.328	140 888.104	120 552.412	181 390.546
0.7	62 134.256	140 829.825	120 671.064	181 260.850
0.8	62 213.564	140 679.105	120 847.990	181 100.023
0.9	62 294.808	140 563.511	120 894.808	180 990.105
1.0	62 407.004	140 428.425	121 066.685	180 816.415

表 9　IEEE 30 节点系统取不同 *w* 值(0~1.0)所对应的污染排放量和燃料费用优化结果
Tab. 9　Emissions and fuel cost *w* varies from 0.0 to 1.0 in increments of 0.1 for IEEE 30-bus system

w	Without security region constraints		With security region constraints	
	Emissions/(kg/h)	Fuel cost/($/h)	Emissions/(kg/h)	Fuel cost/($/h)
0.0	68 832.562	144 155.118	137 553.132	184 220.646
0.1	68 868.992	144 119.998	137 621.588	183 671.413
0.2	68 895.476	144 080.525	137 692.999	183 612.122
0.3	68 924.296	144 016.932	137 771.638	183 553.986
0.4	68 956.682	143 983.182	137 885.791	183 494.877
0.5	69 000.214	143 929.328	137 972.292	183 425.596
0.6	69 034.212	143 859.843	138 076.199	183 355.723
0.7	69 070.286	143 767.421	138 202.743	183 304.968
0.8	69 095.748	143 714.133	138 315.225	183 183.602
0.9	69 147.216	143 642.866	138 403.906	183 102.569
1.0	69 209.872	143 520.559	138 511.936	182 991.546

that while fuel cost decreases continuously similar to the case without security constraints for the two systems, emissions increase. Thus fuel cost and emissions are found to be conflict.

Fig. 1 and Fig. 2 show the trade-off curve for IEEE 14-bus system for the complete range of w (0~1.0) with security constraints and without security constraints respectively. The desired optimal operating policies for the 14-bus system occur at the points where w is approximately 0.400 with security constraints and 0.306 without security constraints respectively. At these points, operating the system will result in an emissions of 120 305.303 kg/h and a generation cost of 181 600.778 $/h with security constraints, and emissions of 61 871.145 kg/h and a generation cost of 141 280.250 $/h without security constraints respectively.

For 30-bus system, Fig. 3 and Fig. 4 show the trade-off curve with security constraints and without security constraints respectively. The desired optimal operating policies for the 30-bus system occurred at the points where w is approximately 0.437 with security constraints and 0.329 without security

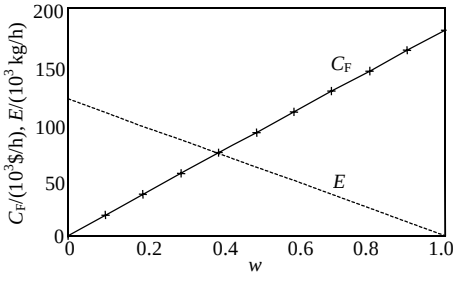

图 1 IEEE 14 节点系统考虑安全性约束时的污染排放量和燃料费用曲线

Fig. 1 Trade-off curve for IEEE 14-bus system with SR constraints

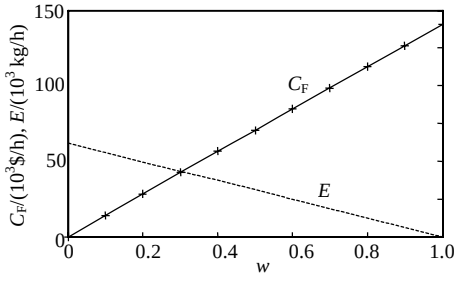

图 2 IEEE 14 节点系统不考虑安全性约束时的污染排放量和燃料费用曲线

Fig. 2 Trade-off curve for IEEE 14-bus system without SR constraints

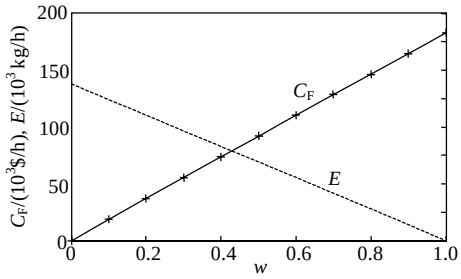

图 3 IEEE 30 节点系统考虑安全性约束时的污染排放量和燃料费用曲线

Fig. 3 Trade-off curve for IEEE 30-bus system with SR constraints

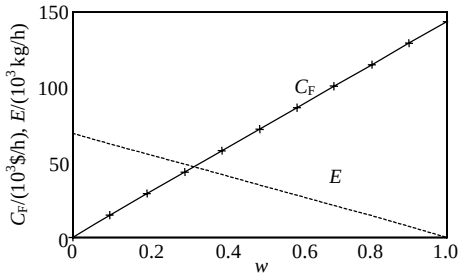

图 4 IEEE 30 节点系统不考虑安全性约束时的污染排放量和燃料费用曲线

Fig. 4 Trade-off curve for IEEE 30-bus system without SR constraints

constraints respectively. At these points, operating the system will result in an emissions of 137 890.197 kg/h and a generation cost of 183 481.787 $/h with security constraints and emissions of 68 931.269 kg/h and a generation cost of 144 006.329 $/h without security constraints respectively.

5 CONCLUSIONS

The formulation of optimal hydrothermal power flow problem suggested in this paper can consider transmission line thermal limits, transient stability constraints, static voltage stability constraints, transmission loss and the minimum emissions objective in the classic minimum fuel cost objective.

The distribution factors for expressing transmission loss are generated efficiently and accurately from available base load flow information using a perturbation technique.

The application of the novel initial guesses to the proposed method can represent the fastest convergence property and require smallest CPU time. The trade-off curves obtained demonstrate how an operational policy may be chosen as a compromise

between fuel cost and emissions.

The proposed method minimizes the objective function for a whole period of time of different interval and system demands (system load points) while satisfying all constraints effectively and should therefore appeal to the utilities for online application.

REFERENCES

[1] Dhillon J S，Parti S C，Kothari D P．Fuzzy decision-making in the stochastic multiobjective short-term hydrothermal scheduling[J]．IEE Proceedings-Generation，Transmission and Distribution，2002，149(2)：191-200．

[2] Gil E，Bustos J，Rudnick H．Short-term hydrothermal generation scheduling model using a genetic algorithm[J]．IEEE Transactions on Power Systems，2003，18(4)：1256-1264．

[3] El-Hawary M E，Ravindranath K M．Hydro-thermal power flow scheduling accounting for head variations[J]．IEEE Transactions on Power Systems，1992，7(3)：1232-1238．

[4] Yang JinShyr，Chen Nanming．Short-term hydrothermal coordination using multi-pass dynamic programming[J]．IEEE Transactions on Power Systems，1989，4(3)：1050-1056．

[5] Wong K P，Wong Y W．Short-term hydrothermal scheduling part．I：Simulated annealing approach，part II：parallel simulated annealing approach[J]．IEE Proceedings，Generation，Transmission and Distribution，1994，141(5)：497-506．

[6] Bath S K，Dhillon J S，Kothari D P．Fuzzy satisfying stochastic multi-objective generation scheduling by weightage pattern search methods[J]．ELSEVIER Electric Power Systems Research，2004，69(2-3)：311-320．

[7] Sinha N，Chakrabarti R，Chattopadhyay P K．Fast evolutionary programming techniques for short-term hydrothermal scheduling[J]．IEEE Transactions on Power Systems，2003，18(1)：214-220．

[8] El-Hawary M E，Landrigan J K．Optimum operation of fixed-head hydro-thermal electric power systems：powell’s hybrid method versus newton-raphson method[J]．IEEE Transactions on Power Apparatus and Systems，1982，101(3)：547-553．

[9] Wei H，Saraki H，Kubokawa J．A decoupled solution of hydrothermal optimal power flow problem by means of interior point method and network programming[J]．IEEE Transactions on Power Systems，1998，13(2)：286-293．

[10] Hau Wei，Hiroshi Sasaki，Junji Kubokawa，et al．Large scale hydrothermal optimal power flow problems based on interior point nonlinear programming[J]．IEEE Transactions on Power Systems，2000，15(1)：396-403．

[11] Mbamalu G A N，Ferial，El-Hawary M E．Effects of load modeling on minim El-Hawary um loss，minimum emission，and multiple-objective optimal hydrothermal power flow[J]．ELSEVIER Electric Power Systems Research，1995，34(2)：97-108．

[12] Talaq J H，Ferial，El-Hawary M E．A Summary of environmental economic dispatch algorithms[J]．IEEE Transactions on Power Systems，1994，9(3)：1508-1516．

[13] Dhillon J S，Kothari D P．The surrogate worth trade-off approach for multiobjective thermal power dispatch problem[J]．ELSEVIER Electric Power Systems Research，2000，56(2)：103-110．

[14] Chen JiannFuh，Chen HuangCheng，Hua ChingLien，The uniqueness of the local minimum for power economic dispatch problems [J]．ELSEVIER Electric Power Systems Research，1995，32(3)：187-193．

[15] Nanda A，Uy D，Crow M，et al．A powerful and computational efficient algorithm for transmission loss calculation[C]．The IEEE Power Engineering Society，Transmission and Distribution Conference，Chicago，IL，USA，1994．

[16] Chung Changyung，Yang Weitzen，Chang Liuchun，A new method for calculating loss cosfficients[J]．IEEE Transactions on Power Systems，1994，9(3)：1665-1671．

[17] 哈比比，余贻鑫．基于安全域的电力系统有功及无功优化[J]．中国电机工程学报，2006，26(12)：1-10．
Binkou A，Yu Yixin．Security region based real and reactive optimization of power systems[J]．Proceedings of the CSEE，2006，26(12)：1-10(in Chinese)．

[18] 韩琪，余贻鑫，李慧玲，等．电力系统注入空间静态电压稳定域边界的实用表达式[J]．中国电机工程学报，2005，25(5)：8-14．
Han Qi，Yu Yixin，Li Huiling，et al．A practical boundary expression of static voltage stability region in injection space of power systems[J]．Proceedings of the CSEE，2005，25(5)：8-14 (in Chinese)．

[19] 李慧玲，余贻鑫，韩琪，等．割集功率空间上静态电压稳定域的实用边界[J]．电力系统自动化，2005，29(4)：18-23．
Li Huiling，Yu Yixin，Han Qi，et al．Practical boundary of static voltage stability region in cut-set power space of power systems [J]．Automation of Electrical Power Systems，2005，29(4)：18-23 (in Chinese)．

[20] Yu Yixin，Feng Zhaofei．Application of dynamic equivalents in determining practical dynamic security region[C]．IEEE/PES Transmission and Distribution Conference and Exhibition：Asia and Pacific，Dalian，China，2005．

[21] Wood A J，Wollenberg B F．Power generation，operation and control [M]．New York：John Wiley & Sons，1996．

[22] Wai Y Ng．Generalized generation distribution factors for power system security evaluations[J]．IEEE Transactions on Power Apparatus and Systems，1981，PAS-100 (3)：1001-1005．

收稿日期：2007-11-03。

作者简介：

哈比比(1963—)，男，博士研究生，主要研究方向为电力系统安全与稳定，habibbinkou@yahoo.fr；

余贻鑫(1936—)，男，中国工程院院士，教授，博士生导师，主要从事电力系统安全性和稳定性以及配网规划方面的教学和研究。

(责任编辑　王剑乔)